



NONLINEAR ANALYSIS OF REINFORCED CONCRETE VIERENDEEL TRUSSES

Dr. Qassim M. Shaker

Email: qasimm.alabbasi@uokufa.edu.iq

Dr. Hayder H. H. Kamonna

E mail: kamonnahh@yahoo.com

Dr. Mohammed A. Attia

E mial: mo_attia@yahoo.com

University of Kufa \ College of Engineering /Civil Department

(Received:22/10/2011 ; Accepted :20/2/2012)

Abstract:

This paper considers the practical application of nonlinear models in the analysis of Vierendeel truss. Results of some analyses performed using the reinforced concrete model of the general purpose finite element code ANSYS which had been obtained from previous works are presented and discussed. An incremental loading procedure is adopted following step by step nonlinear response. ANSYS program has the ability to use conventional Newton-Raphson (N-R), full (N-R) and modified (N-R) Procedure to perform the analysis process. The defaulted choice (program chosen) is used in this work which allows for automatically chosen of the most suitable method. Number of sub-steps for each case was changed until converged solution and full load deflection curve were obtained. Good agreement with the experimental tests of some previous studies was obtained using ANSYS solution. The maximum difference with the experimental test is found to be less than 10%. The effect of shear transfer coefficients of an open and a closed cracks are also studied. It was found that changing shear transfer coefficient of an open crack has more effect than changing of closed crack on the behavior of Vierendeel truss.

Key words: Vierendeel Truss, Nonlinear Analysis, Finite Element Analysis.

التحليل اللا خطي للمسلمات الخرسانية المسلحة نوع فرندييل

المدرس الدكتور قاسم محمد شاكر المدرس الدكتور حيدر حسين حريب كمونة المدرس الدكتور محمد عبد عطية
جامعة الكوفة/ كلية الهندسة/ قسم الهندسة المدنية

الخلاصة:

يتضمن هذا البحث دراسة نظرية لاستخدام التحليل اللا خطي لتحليل المسلمات الخرسانية المسلحة نوع فرندييل. إذ تم تحليل عدد من الأمثلة العملية التي تم الحصول عليها من دراسات سابقة. تم استعمال طريقة تجزئة الأحمال المطلقة وتسليطها على مراحل. لبرنامج ANSYS القابلية على استخدام طرق نيوتن-رافسن الأعتيادية والكلية والمطورة. في هذه الدراسة أعتمد على اختيار الطريقة المناسبة أوتوماتيكيا من قبل البرنامج نفسه، إذ إن للبرنامج القابلية لاختيار الطريقة المناسبة لإتمام عملية التحليل والحصول على (converged solution). لوحظ انه يجب تقسيم الحمل المسلط بنسب كي تعطي (converged solution) وبالتالي منحنى حمل-هطول كامل. وقد وجد إن هناك توافق جيد بين نتائج الفحص العملية مع النتائج التي تم الحصول عليها من خلال البرنامج (ANSYS) عند تمثيل المنشآت أعلاه بصورة مناسبة مع اختيار قيم مناسبة لعوامل انتقال القص. حيث كان مقدار انحراف النتائج النظرية عن نظيرتها العملية لا يتجاوز ١٠%. كذلك تم دراسة تأثير عوامل انتقال القص للشقوق المفتوحة (المتصلة) والمغلقة، وقد، وجد إن عوامل انتقال القص للشقوق المفتوحة ذات تأثير اكبر على سلوك المنشآت الخرسانية المسلحة نوع فرندييل منه في حالة تغير عوامل انتقال القص للشقوق المغلقة.

الكلمات الدالة: المسلمات الخرسانية، التحليل اللاخطي، طريقة العناصر المحددة.

1. INTRODUCTION

In 1896 professor Arthur Vierendeel developed a rigid frame with open web girders having rigid joints, comprising of a top and bottom chord with vertical members between the top and bottom booms. This type of open frame is popularly known as Vierendeel girders whose experimental work still forms the basis of their design. The prominent feature of the Vierendeel girder being the absence of diagonal members and the frame depends on the rigidity of the joints for stability (Raju 1986).

A **Vierendeel bridge** is a bridge employing a Vierendeel truss. Such trusses do not have the usual triangular voids seen in a pin-joint truss bridge, rather employing rectangular openings and rigid connections in the elements, which (unlike a conventional truss) must also resist substantial bending forces. Owing to a lesser economy of materials and the difficulty of design before the advent of computers, this truss is rarely used in bridges outside Belgium. The form is more

commonly employed in building structures where large shear walls or diagonal elements would interfere with the building's aesthetics or functionality.

Vierendeel girders are usually subjected to bending while the individual members in it are subjected to bending moments and shear force in addition to direct tension or compression. The joints may be heavy, but the absence of diagonals makes this form suitable for storey-height construction. Using standard computer programs, the analysis is not difficult, but the resulting joints are often very heavy in appearance. However the system does allow full storey-height construction without obstruction to openings. Clearly in this situation the verticals would be at column positions. It is common to see this type of truss in the walkways, for instance at airports. This is because the height available relative to the span reduces the boom forces and moments and eases the problem of forming the joints. Vierendeel girders can be used vertically (to resist horizontal loads). While the descriptions so far had concentrated on the truss spanning horizontally, it is by no means necessary and often (particularly with Vierendeels) the truss spans vertically.

Vierendeel girders are used in structures where free unobstructed space is required between the top and bottom chords such as in clerestory lighting in churches and also for main girders in factories and ware house sheds. Vierendeel girders have widely used in Europe and particularly in Belgium where pioneering work on this type of girders were made. The various types of Vierendeel girders used in practice are shown in Fig.1 (Raju 1986).

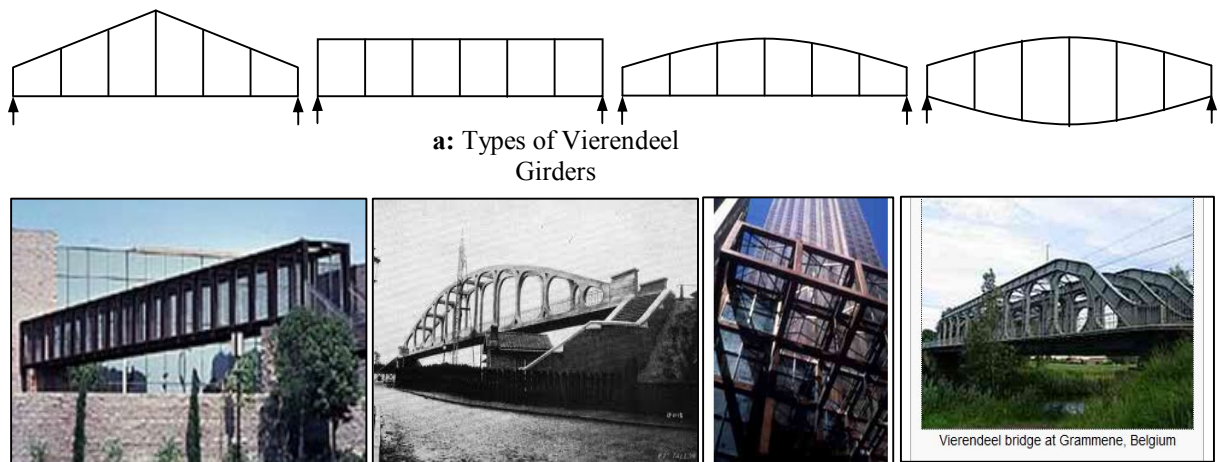


Fig. 1: Types and practical applications of

In 1980 Zhilin discussed the shear strength of the lower chord of the reinforced concrete and prestressed concrete Vierendeel truss. He found that, the lower chord of a Vierendeel truss, when loaded, is subjected to the combined action of prestressed compression, large axial load, moment and shear. On the basis of these experimental data, Zhilin derived the practical formula for calculation of shear of the lower chord of the truss, taking into account the influence of the prestressed compression and longitudinal tension. The calculated results were in good agreement with the test results.

Zhaohul et. al. (in 2004) studied Vierendeel truss, lower transfer beam and upper suspension beam, for portal of Shenhen University Science and Technology building, The results showed that the Vierendeel portal structure has better seismic performance as it is beneficial for smoothing the sudden change of stiffness and mass concentration and reducing high stress concentration in support as well as enhancing the ductility of the portal structure. The influences of connected floor stiffness and long term stiffness degradation of reinforced concrete members' on the whole portal structure were also investigated. The improved joint detail design, crack control design for reinforced concrete members, and special construction method for this structure are put forward as well.

Combined with actual an engineering pseudo-dynamic test of a prestressed part shaped steel reinforced concrete laminated Vierendeel truss transfer storey structure is conducted by Guoliang et. al (2001). Nonlinear dynamic analysis of the specimen was made, and the results indicated that the theoretical curve were in good agreement with the experimental ones. Also the design suggestions of the transfer storey were put forward.

2. MATERIAL CONSTITUTIVE RELATIONS

2.1 Concrete in Compression

The behavior of concrete in compression can be simulated in ANSYS program by an elasto-plastic work hardening model followed by a perfectly plastic response, which is terminated at the onset of crushing.

In the present study, the concrete is assumed to be homogeneous and initially isotropic; the adopted stress-strain relation is based on work done by Desayi and Krishnan (Saenz and Luis, 1964).

The compressive uniaxial stress-strain relationship for concrete model was obtained by using the following equations to compute the multilinear isotropic stress-strain curve for the concrete.

$$f_c = \varepsilon E_c \quad \text{for} \quad 0 \leq \varepsilon \leq \varepsilon_1 \quad (1)$$

$$f_c = \frac{\varepsilon E_c}{1 + (\varepsilon/\varepsilon_0)^2} \quad \text{for} \quad \varepsilon_1 \leq \varepsilon \leq \varepsilon_0$$

(2)

$$f_c = f'_c \quad \text{for} \quad \varepsilon_0 \leq \varepsilon \leq \varepsilon_{cu} \quad (3)$$

and

$$\varepsilon_1 = 0.3 f'_c / (E_c) \quad (\text{Hooke's law})$$

(4)

$$\varepsilon_0 = 2 f'_c / (E_c) \quad (5)$$

where

f_c = stress at any strain ε , MPa

ε = strain at stress f

ε_0 = strain at ultimate compressive stress f'_c and

E_c = concrete elastic modulus, MPa

The multilinear curves were used to help with convergence of the nonlinear solution algorithm.

Fig. 2 is adopted in the present study to represent the behavior of concrete in compression.

2.2. Tensile behavior of concrete

Until the crack, initial tangent modulus E_c is used to find the maximum positive (tensile) stress. After concrete cracking takes place, a smeared model is used to represent the discontinuous macro crack behavior. This cracked concrete can still carry some tensile stress perpendicular to the crack, which is termed tension stiffening. The tension stiffening factor (α_m Fig. 3) was assumed 0.6 in this study. In this work, a simple descending line is used to model this tension stiffening phenomenon as shown in Fig. 3. The default value of the strain ε^* (ε^* is assumed in this work equal six times ε_t , SAS ANSYS 10 (2005)) at which the tension stiffening stress reduced to zero is $\varepsilon^* = 0.002$. In Fig. 3, E_c and E_t are the modulus of elasticity of tensile concrete between zero to fracture strain and fracture strain to ε^* respectively. f'_t is the maximum stress at fracture of concrete, which has corresponding strain ε_t (Chen and Saleeb 1981).

2.3 Modeling of Crack

In the concrete, when the tensile stress in the principal direction exceeds the tensile strength, f'_t , of concrete, the tensile failure would occur (Desai et al. 2002). After the crack forms, both normal and shear stiffness are reduced.

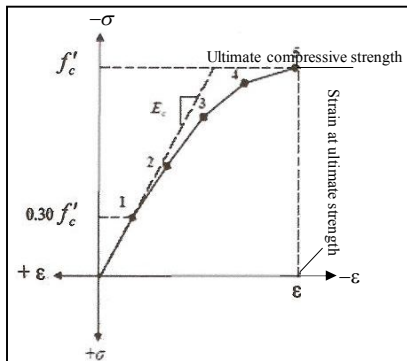


Fig. 2: Uniaxial Stress-Strain Curve for Concrete

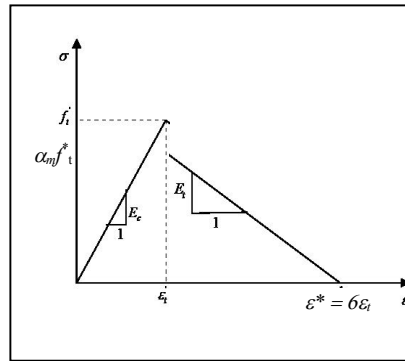


Fig. 3: Tension Stiffening Model

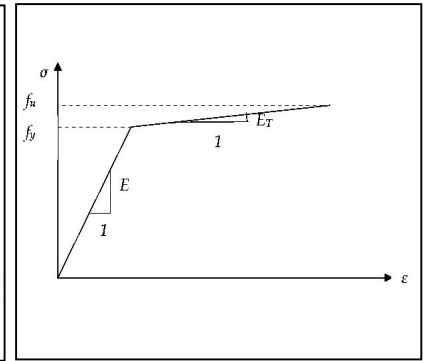


Fig. 4: Uniaxial Stress-Strain Relation for Steel

2.4 Steel reinforcing bars

The stress-strain curve of the reinforcing bars is assumed to be elastic up to the steel yield stress (f_y) followed by linear hardening up to the steel ultimate strength (f_u) as shown in Fig. 4. The dowel action of the reinforcing steel is neglected and the bond between steel and concrete is assumed to remain perfect.

3. APPLICATIONS:

3.1 Details of Vierendeel Trusses Considered in the Presented Study:

The numerical analyses were carried out on three simply supported Vierendeel trusses which were tested by Alwash (1995). The dimensions of the trusses are in Fig. 5. The trusses were constructed with overall length of 4.00 m giving a span of 3.85 m. the width of each truss is 15 cm. the members of all trusses have the same main reinforcement consisting of four deformed bars with 12 mm diameter. The bars were equally distributed on member section (max. percentage of reinforcement equal 2.01%). Ties (lateral reinforcement) were distributed in each member of each truss as shown in Fig. 5 using plain bars of 8 mm diameter. Each truss was loaded by one concentrated load at mid span of the upper chord. The average compressive

strength of concrete are listed in table 1 and the strength properties of the used steel reinforcement are given in table 2.

Table 1: Average compressive strength of concrete:

Model No.	Average cube strength N/mm ²
A ₁	40.35
A ₂	34.81
A ₃	32.57

Table 2: Strength properties of the used steel reinforcement:

Bar diam.	Yield strength N/mm ²	Ultimate strength N/mm ²	Uses
φ 12 mm	483	693	Main Reinf.
φ 8 mm	318	418	Ties

3.2 ANSYS Finite Element Model

The FEA calibration study included modeling a Vierendeel truss with the dimensions and properties as previously mentioned. Due to the symmetry of girders and loading, the symmetry was utilized in the FEA; only one quarter of the girder was modeled.

3.2.1 Element Types

A solid element, **SOLID65** (Fig. 6) is used to model the concrete in ANSYS. The solid element has eight nodes with three degrees of freedom at each node, translations in the nodal *x*, *y*, and *z* directions. The element is capable of plastic deformation, and cracking in three orthogonal directions. A **LINK8** (Fig. 7) element is used to model the steel reinforcement. Two nodes are required for this element. At each node, degrees of freedom are identical to those for the SOLID65. The element is also capable of plastic deformation.

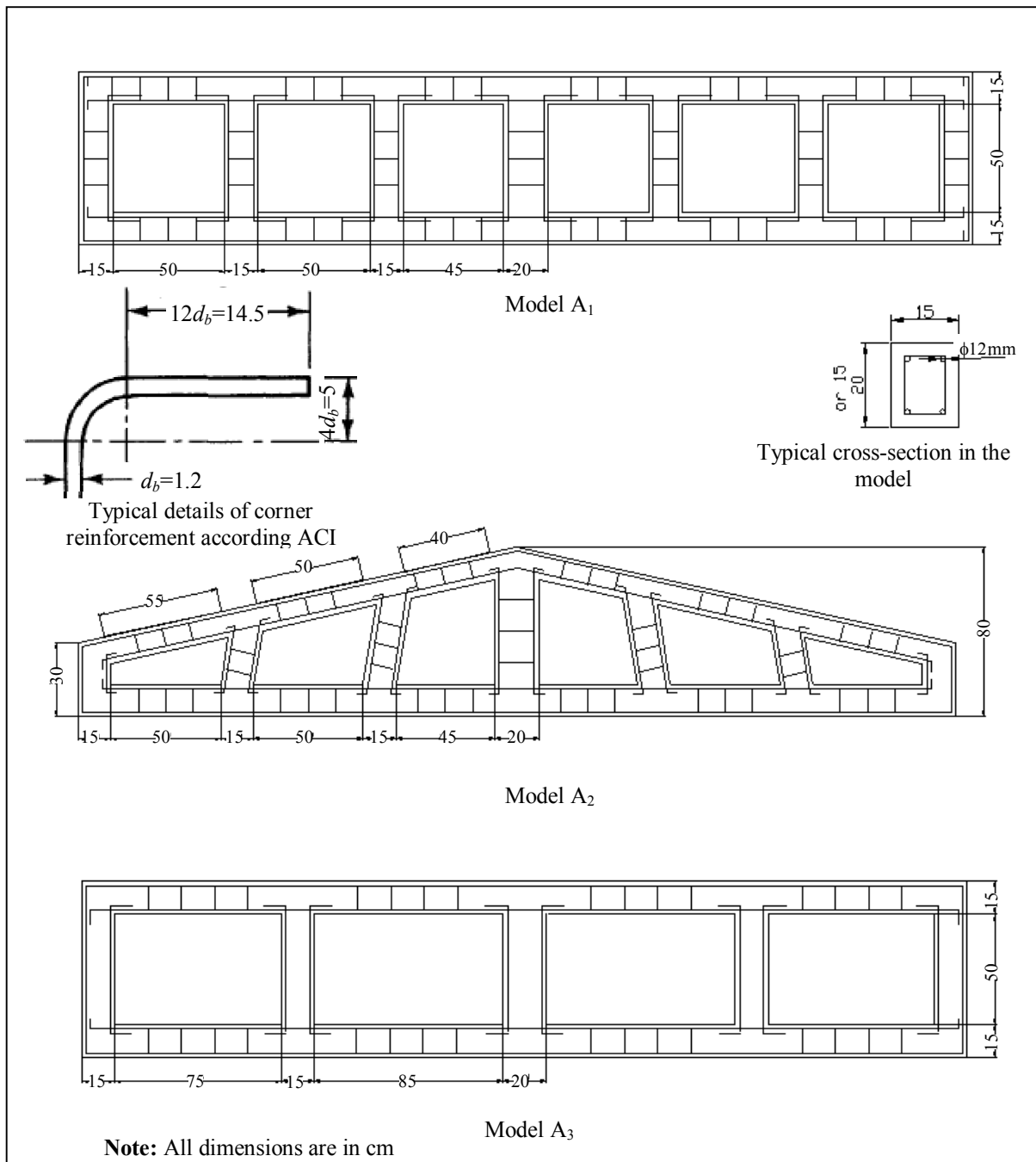


Fig. 5: Dimension and details of reinforcement for tested models

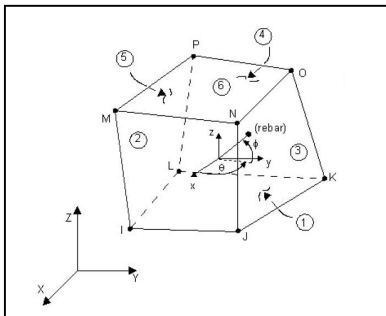


Fig. 6: Solid65 Element (SAS 2005)

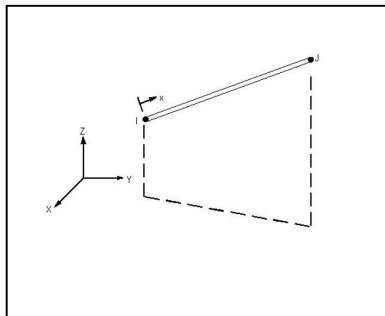


Fig. 7: Solid8 Element (SAS 2005)

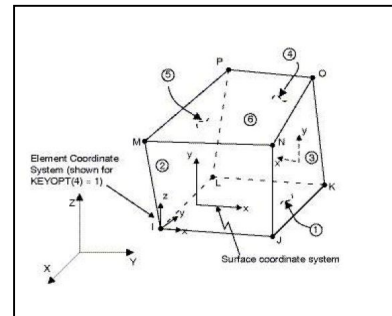


Fig. 8: Solid45 Element (SAS 2005)

A solid element, **SOLID45** (Fig. 8) is used to model the loading and support plates. The solid element has also eight nodes with three degrees of freedom at each node, translations in the nodal x, y, and z directions.

3.2.2 Real Constants

The real constants for this model are shown in Table 3. It can be noted that the individual elements contain different real constants. No real constant set exists for the Solid45 element.

Real Constant Set 1 is used for the Solid65 element. It requires real constants for rebar assuming a smeared model. Values can be entered for Material Number, Volume Ratio, and Orientation Angles. The material number refers to the type of material for the reinforcement. The volume ratio refers to the ratio of steel to concrete in the element. The orientation angles refer to the orientation of the reinforcement in the smeared model. ANSYS (SAS 2005) allows the user to enter three rebar materials in the concrete. Each material corresponds to x, y, and z directions in the element (Fig. 7). The reinforcement has uniaxial stiffness and the directional orientation is defined by the user. In the present study the beam is modeled using discrete reinforcement. Therefore, a value of zero was entered for all real constants which turned the smeared reinforcement capability of the Solid65 element off.

Table 3: Real Constant Typical Model

Real constant set	Element type	Constant			
			Real constant for Rebar1	Real constant for Rebar2	Real constant for Rebar3
1 (concrete)	Solid 65	Material number	0	0	0
		Volume Ratio	0	0	0
		Orientation Angle	0	0	0
		Orientation Angle	0	0	0
2 (main reinforcement)	Link8	Cross-sectional area(mm ²)	113		
		Initial strain(mm/mm)	0		
3 (secondary reinforcement)	Link8	Cross-sectional area(mm ²)	50.2		
		Initial strain(mm/mm)	0		
4 (main reinforcement corner)	Link8	Cross-sectional area(mm ²)	226		
		Initial strain(mm/mm)	0		

Real Constant Sets 2 and 3 are defined for the Link8 element. Values for cross-sectional area and initial strain were entered. Cross-sectional areas in sets 2 and 3 refer to the reinforcement main and secondary reinforcement respectively. While

set 4 refers to the reinforcement at corners at which anchors were found since doubling the value of area is simpler than doubling elements at these locations. A value of zero was entered for the initial strain because there is no initial stress in the reinforcement.

3.2.3 Material Properties

Parameters needed to define the material models can be found in Table 4. As seen in Table 4, there are multiple parts of the material model for each element. Material Model Number 1 refers to the Solid65 element. The Solid65 element requires linear isotropic and multilinear isotropic material properties to properly model concrete. The multilinear isotropic material uses the Von Mises failure criterion along with the Willam and Warnke (1974) model to define the failure of the concrete. EX is the modulus of elasticity of the concrete (E_c), and PRXY is the Poisson's ratio (ν). The modulus was based on the equation (ACI 318 2005):

$$E_c = 4750\sqrt{f'_c} \quad (6)$$

The compressive uniaxial stress-strain relationship for the concrete model was obtained using the equations in section 2 to compute the multilinear isotropic stress-strain curve for concrete.

A shear transfer coefficient β_t (constant c_1) is introduced which represents a shear strength reduction factor for those subsequent loads which induce sliding (shear) across the crack face. If the crack closes, then all compressive stresses normal to the crack plane are transmitted across the crack and only a shear transfer coefficient β_c (constant c_2) for a closed crack is introduced (SAS 2005).

Typical shear transfer coefficients range from 0.0 to 1.0, with 0.0 representing a smooth crack (complete loss of shear transfer) and 1.0 representing a rough crack (no loss of shear transfer). The shear transfer coefficients for open and closed cracks were determined using the work of Kachlakev, et al. (2001) as a basis (Anthony 2004). The uniaxial crushing stress in this model was based on the uniaxial unconfined compressive strength (f'_c).

Material Model Number 2 refers to the Solid45 element. The Solid45 element is being used for the steel plates at loading points and supports on the beam. Therefore, this element is modeled as a linear isotropic element with a modulus of elasticity for the steel ($E_s=20000$ MPa), and Poisson's ratio (0.3).

Material Model Number 3 refers to the Link8 element. The Link8 element is being used for all the steel reinforcement in the beam and it is assumed to be bilinear isotropic. Bilinear isotropic material is also based on the Von Mises failure criteria. The bilinear model requires the yield stress (f_y), as well as the hardening modulus of the steel to be defined. The yield stress was defined as 383 MPa and 318 MPa for main and secondary reinforcement respectively. The hardening modulus was 0.0 MPa.

3.2.4 Modeling Methodology

By taking advantage of the symmetry of the girders, a quarter of the full girder is used for modeling with proper boundary conditions. This approach reduces computational time and computer disk space requirements significantly. Ideally, the bond strength between the concrete and steel reinforcement should be considered. However, in this study, perfect bond between materials is assumed. Plates and supports were modeled using solid45 element. While Solid 65 elements were used to model reinforced concrete specimen. And Link8 elements were used to create the main and secondary reinforcement.

Table 4: Material Models for Typical Model

Material Model Number	Element Type	Material Properties						
		Linear Isotropic		Multilinear Isotropic		Concrete		
1	Solid65	EX	23923.61 MPa		strain	stress	ShrCf-Op(c_1)	0.9
		PRXY	0.2	Point1 (Fig. 2) [*]	0.0004052	9.7	ShrCf-Cl (c_2)	0.1
				Point2	0.001	22.26	UnTensSt (c_3)	3.228
				Point3	0.0015	27.50	UnCompSt (c_4)	32.28
				Point4	0.002	31.71	BiCompSt (c_5)	0
				Point5	0.0025	39.64	HydroPrs (c_6)	0
				Point6	0.003	32.28	BiCompSt (c_7)	0
							UnTensSt (c_8)	0
							TenCrFac (c_9)	0.6 (effective if $k_7=1$)
		2	Solid45	Linear Isotropic				
EX	200000 MPa							
PRXY	0.3							
3	Link8 (Main reinforcement)	Linear Isotropic		Bilinear Isotropic				
		EX	200000 MPa	Yield Stress	383 MPa			
		PRXY	0.3	Tang Mod	0 MPa			
4	Link8 (secondary reinforcement)	Linear Isotropic		Bilinear Isotropic				
		EX	200000 MPa	Yield Stress	318 MPa			
		PRXY	0.3	Tang Mod	0 MPa			

To obtain good results from the Solid65 element, the use of a rectangular mesh is recommended. Therefore, the mesh was set up such that square or rectangular elements were created (Fig. 8). Creating of nodes with acceptable distance (max. distance 5 mm) was firstly done then connecting those nodes by suitable elements. The necessary mesh attributes need to be set before each type of elements is created.

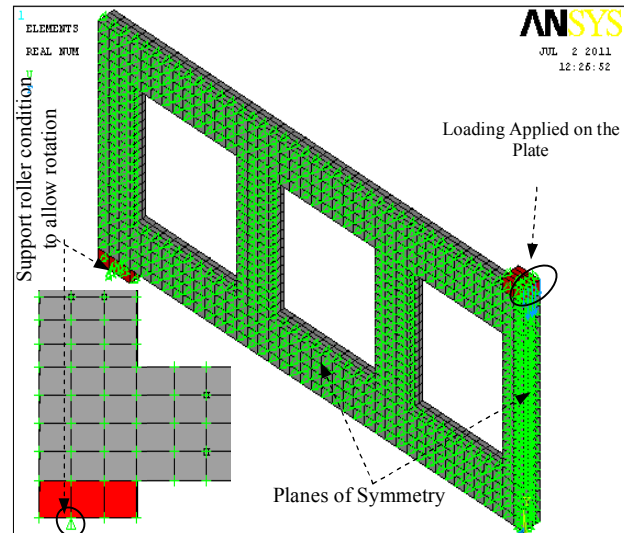


Fig. 9: Boundary Conditions of a Typical Beam (A₁)

3.2.5 Loads and Boundary Conditions

Displacement boundary conditions are needed to constrain the model to get a unique solution. To ensure that the model acts the same way as the experimental beam boundary conditions need to be applied at points of symmetry, and where the supports and loadings exist. The boundary conditions for both planes of symmetry are shown in Fig. 9.

The support was modeled in such a way that a roller was created. A single line of nodes on the plate were given constraint in the UY, and UZ directions, applied as constant values of 0. By doing this, the beam will be allowed to rotate at the support.

The force, P, applied at the steel plate is applied across the entire centerline of the plate.

3.2.6 Analysis Type

The finite element model for this analysis is a simple span of girder under transverse loading. For the purposes of this model, the Static analysis type is utilized. The Restart command is utilized to restart an analysis after the initial run or load step has been completed. The use of the restart option will be detailed in the analysis portion of the discussion. The Sol'n Controls command dictates the use of a linear or non-linear solution for the finite element model. Typical commands utilized in a nonlinear static analysis are shown in Table 5.

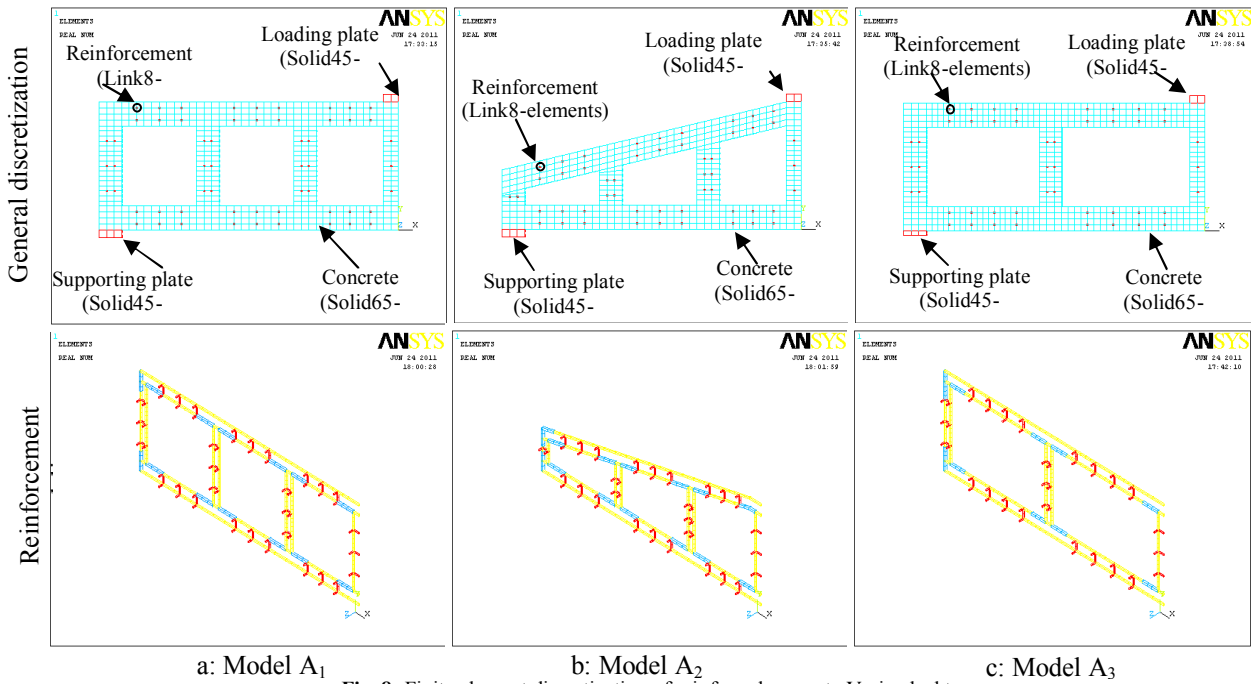


Fig. 8: Finite element discretization of reinforced concrete Veriendeel trusses

Table 5: Commands Used to Control Nonlinear Analysis.

Analysis Options	Small Displacement
Calculate Prestress Effects	No
Time at End of Loadstep	100*
Automatic Time Stepping	On
Number of Substeps	200*
Max no. of Substeps	250*
Min no. of Substeps	10
Write Items to Results File	All Solution Items
Frequency	Write Every Substep

While other commands values are set to ANSYS (SAS 2005) defaults, except the maximum number of iteration which is set to 100 and the convergence criteria which are set to those showing in Table 6.

Table 6: Convergence Criteria

Label	U
Ref. Value	Calculated
Tolerance	0.001
Norm	infinite
Min. Ref.	not applicable

4. RESULTS AND DISCUSSION

Three models of reinforced concrete Vierendeel trusses that were tested by Alwash in 1995 are analyzed by using ANSYS program. Alwash (1995) proposed two methods for analysis of parallel chords Vierendeel trusses with rigid ended vertical members. These methods include derivation of three general equations represent the relation between the redundant unknowns (moment, shear force and axial force at the center of panels). The solving of the derived equations can be handled by using of successive approximation which gives good approximation. The values of panel point (joint) displacement were found by using the direct integration method since the applied forces of all members were determined.

The dimensions and details of these models are illustrated in Fig. 5. Through analysis process the load step size was changed until converge solution obtained. At higher load the convergence criterion was increased and a restart command was used to get full load-deflection curve.

Load-deflection curves of numerical and experimental test of the three models are shown in Fig. 10. It can be seen from Fig. 10 that, at beginning of the loading, numerical analysis gives stiff solution compared with the experimental test. This may be attributes to that at the beginning of the test; the specimen was not completely confirmative, so it gives high displacement at low loads. But as the load increases the specimen will be restricted so the slope of load-deflection curve (stiffness of specimen) may increase. Good agreement with the experimental test was obtained after this stage of loading. Table 7 shows a comparison between experimental ultimate load and those obtained from the analysis by Alwash and present study. The maximum deflection for the experimental work is considered as the reference to establish the comparison in load capacity between the experimental work and present study. It can be seen that the maximum difference in the present study was less than 10%, while the analysis results obtained by Alwash were ranged between (6.8-26.3) %.

Table 7: Comparison between Experimental Ultimate Load and Those Obtained from the Analysis by Alwash and Present Study:

Vierendeel Type	P _{exper.} (kN)	P _{by Alwash.} (kN)	P _{present.} (kN)	% of $\frac{P_{by\ Alwash}}{P_{exper.}}$	% of $\frac{P_{present}}{P_{exper.}}$
A ₁	88	82	94.33	93.2	107.2
A ₂	95	120	87	126.3	91.6
A ₃	54	63	57.17	116.7	105.9

Load-deflection curves including the effect of changing shear transfer coefficients (c_1 and c_2) on the behavior of reinforced concrete Vierendeel truss of model A_1 are shown in Fig. 11. It can be seen by this figure that increasing the value(s) of c_1 and/or c_2 increases the stiffness of the structure. Assuming c_1 constant and changing c_2 has more effect on the behavior of the structure than changing both coefficients or changing c_1 and assuming c_2 constant. More stiff behavior is obtained with low values of c_1 ($c_1=0.05$). The shear transfer coefficients of open and closed cracks were set to such that good agreement with the experimental was obtained. Good agreement with the experimental test was obtained with those values listed in Table 8.

Table 8: coefficients for the open and closed cracks

Model No.	Coefficient for	
A_1	Open crack	0.6
	Close crack	0.05
A_2	Open crack	0.2
	Close crack	0.6
A_3	Open crack	0.4
	Close crack	0.35

Fig. 12 shows the first cracks of each model, cracks at approximately half ultimate load and cracks at ultimate loads. Deformed shapes at ultimate load are also shown in fig.12. Initial crack was happened at load approximately (18.6), (25) and (22.5) percent of the ultimate load for models A_1 , A_2 , and A_3 respectively. First crack initiated at high load in Model A_2 compared to other models. This may be attributed to the absence of that inclined chords which will support some of vertical force as axial compression force in case of horizontal chords. This axial compression force may increase the stiffness of member. So this will delay initiating of cracks and also increase the ultimate load and decrease the total amount of material (gross weight of structure). It can be noted also from Fig. 12 that the distribution of cracks are at corners because of concentration of stress at these locations (rigid-joints). At ultimate loads it can be observed that the cracks in the lower chords are higher than the upper chords and this is due to the high tensile stress initiated on the lower chord compared to those in the upper chords.

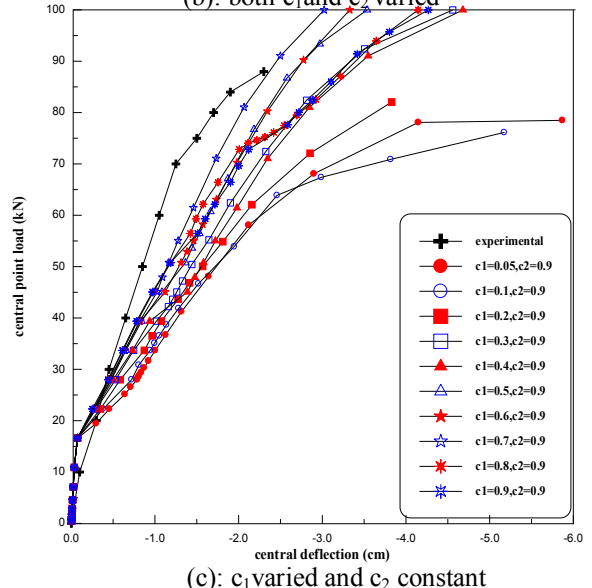
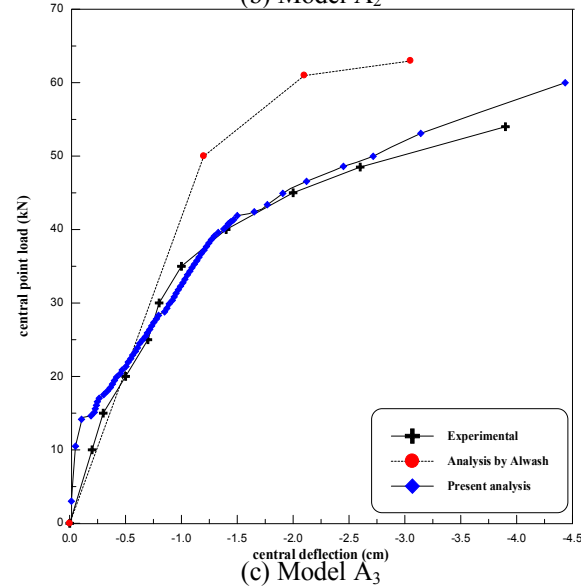
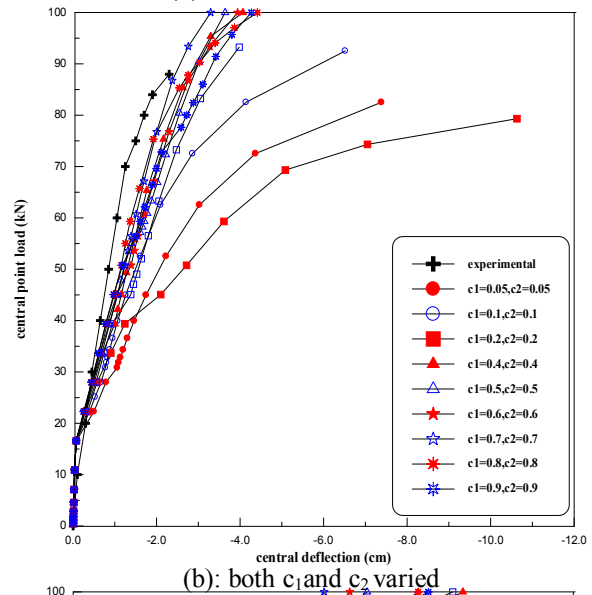
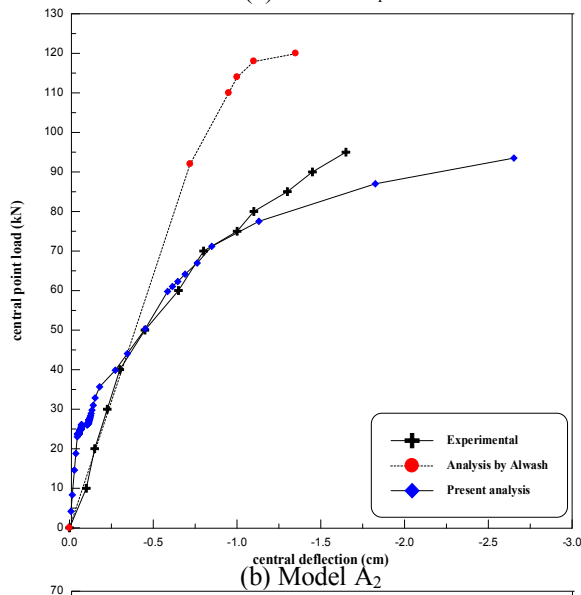
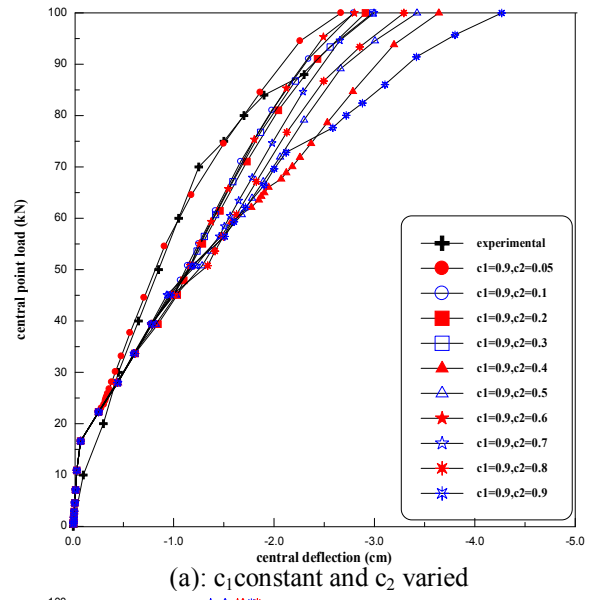
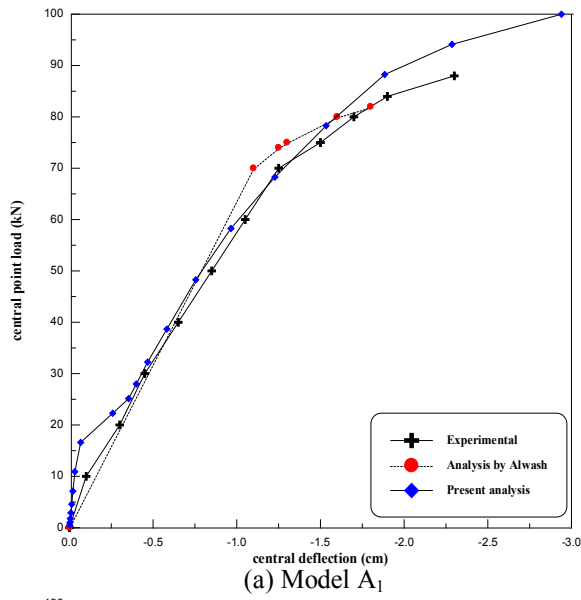


Fig. 10: Experimental and numerical load-deflection

Fig. 11: Load-deflection curves for reinforced concrete Veriendeel truss of model A₁ with changing the shear transfer coefficient for an open crack (c_1) and closed crack c_2

5. CONCLUSIONS

A number of conclusions can be drawn from this study.

1. Full load deflection curves can be obtained by ANSYS program in the analysis of reinforced concrete Veriendeel truss if adequate representation of the structure is provided with suitable no. of sub-steps.
2. Shear transfer coefficients for an open and closed cracks has a considerable effect on the stiffness of such structures. It was also found that these coefficients for an open crack have more effect of those of closed cracks.
3. The first crack in the reinforced concrete Vierendeel truss with inclined chord appears at high load compared with structure having horizontal chord.
4. Number of voids has a considerable effect on ultimate strength of Veriendeel truss. It was found that the ultimate strength increases with increasing number of voids in the structures having the same span.
5. Good agreement with the experimental test can be obtained if a good representation is made for the structure with suitable selection of shear transfer coefficient. The maximum difference with the experimental test was less than 10%.

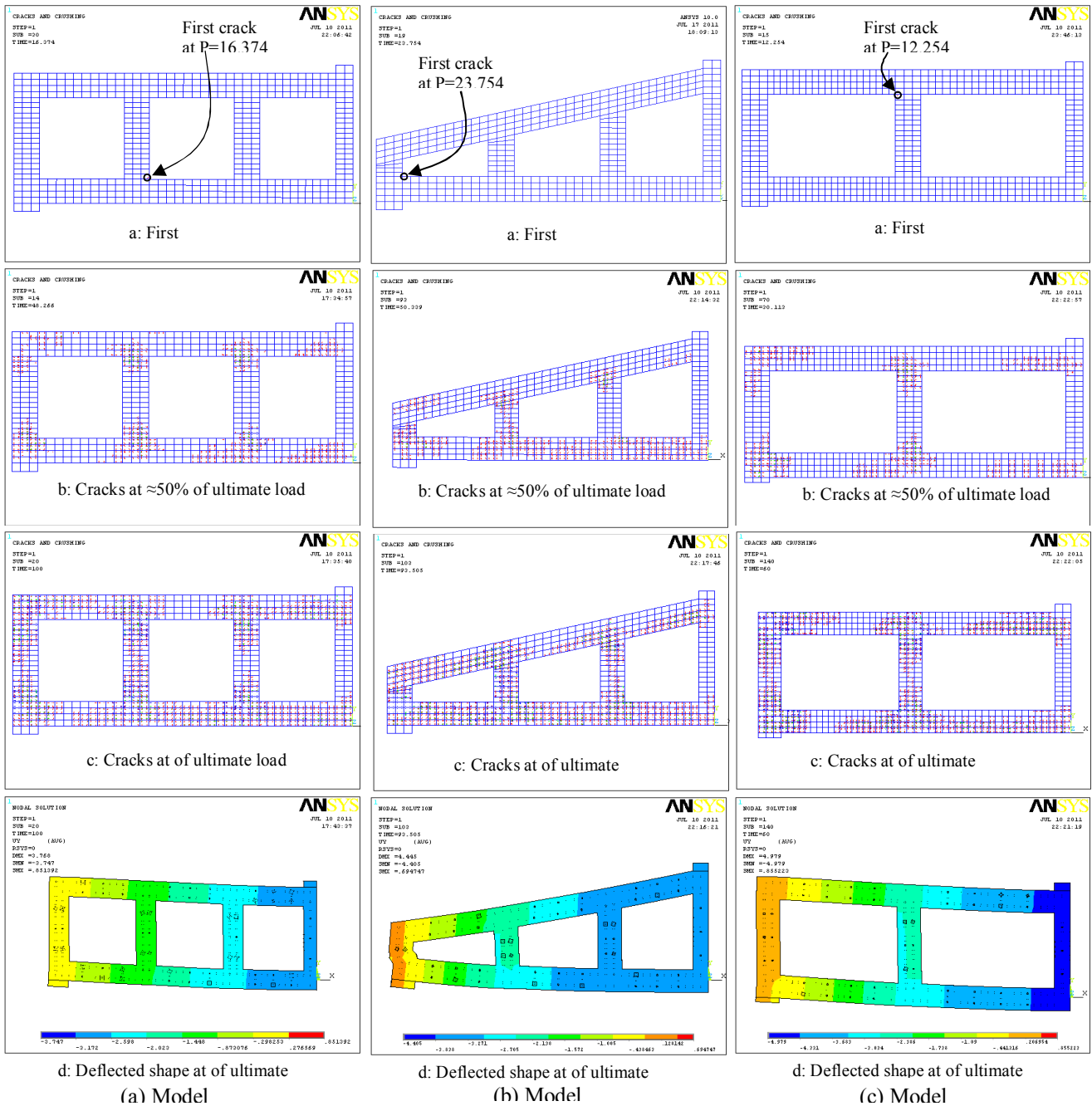


Fig. 12: Cracks and deflected shape of reinforced concrete Vierendeel truss

6. REFERENCES

ACI Committee 318, 2008 "*Building Code Requirements for Structural Concrete (318-08) and Commentary (318M-08)*", American Concrete Institute, Farmington Hills, MI.

- Alwash N. A., 1995, "***Nonlinear Behavior an Optimal Design of Reinforced Concrete Veriendeel Trusses***" Ph. D. Thesis University of technology, Baghdad Iraq.
- Anthony J. W., 2004, "***Flexural Behavior of Reinforced and Prestressed Concrete Beams Using Finite Element Analysis***", M. Sc. Thesis, Marquette University, pp. 73.
- Chen, W. F. and Saleeb, A. F., December 1981, "***Constitutive Equations for Engineering Materials***", West Lafayette, Indiana, pp. 580.
- Desai, Y. M.; Mufti, A. A.; and Tadros, G., 2002, "***User Manual for FEM PUNCH, Version 2.0***", ISIS Canada.
- Guoliag, D., Yongsheng, J., Shuting, L., and Chuanguo, F., 2001, "***Experimental Study of Pseudo-Dynamic Seismic Response of Vierendeel Truss Transfer Storey Structure***", Journal of Industrial Construction, Vol. 6.
- Kachlakev D. I., "***Finite Element Analysis and Model Validation of Shear Deficient Reinforced Concrete Beams Strengthened with GFRP Laminates***" California Polytechnic State University, (Cited by Anthony 2004).
- Raju, N. K., 1986, "***Advanced Reinforced Concrete Design***", CBS Puplichers & Distributers", First Edition, PP. 360.
- Saenz, and Luis, P., 1964, "***Discussion of Equation for the Stress-Strain Curve of Concrete' by Prakash Desayi and S. Krishnan***", ACI Journal, V. 61, N. 9, pp. 1229-1235.
- SAS ANSYS 10.0, "***Finite Element Analysis System***", SAS IP, Inc., U.S.A., 2005.
- Willam, K. J., and Warnke, E. P., 1974, "***Constitutive Model for Triaxial Behaviour of Concrete***", ***Seminar on Concrete Structures Subject to Triaxial Stresses***", International Association of Bridge and Structural Engineering Conference, Bergamo, Italy, pp. 174.
- Zhaohul, C., Xueyi, F., Xiangbing, Y., Songliang, C. and Lei, G., 2004, "***Study on Steel Reinforced Concrete Vierendeel Portal Structure- Portal Structure Design of Shenhen University Science and Technology Building***", Journal of Building Structures, Vol. 25, No. 2 pp. 64-71.
- Zhilin, Y. 1980, "***Shear Strength of the Lower Chord of the Reinforced Concrete and Prestressed Concrete Vierendeel Truss (Discussion on Shear Strength of Eccentric Tension Members.***" Journal of Building Structures Vol. 2.